Preparation of high-strength Al–Mg–Si–Cu–Fe alloy via heat treatment and rolling

Chong-yu Liu[1,2,3], *Peng-fei Yu*[1], *Xiao-ying Wang*[1], *Ming-zhen Ma*[1], *and Ri-ping Liu*[1]

1) State Key Laboratory of Metastable Materials Science and Technology, Yanshan University, Qinhuangdao 066004, China

2) Key Laboratory of New Processing Technology for Nonferrous Metal & Materials, Ministry of Education, Guilin University of Technology, Guilin 541004, China

3) College of Materials Science and Engineering, Guilin University of Technology, Guilin 541004, China

Abstract: An Al–Mg–Si–Cu–Fe alloy was solid-solution treated at 560°C for 3 h and then cooled by water quenching or furnace cooling. The alloy samples which underwent cooling by these two methods were rolled at different temperatures. The microstructure and mechanical properties of the rolled alloys were investigated by optical microscopy, scanning electron microscopy, transmission electron microscopy, X-ray diffraction analysis, and tensile testing. For the water-quenched alloys, the peak tensile strength and elongation occurred at a rolling temperature of 180°C. For the furnace-cooled alloys, the tensile strength decreased initially, until the rolling temperature of 420°C, and then increased; the elongation increased consistently with increasing rolling temperature. The effects of grain boundary hardening and dislocation hardening on the mechanical properties of these rolled alloys decreased with increases in rolling temperature. The mechanical properties of the 180°C rolling water-quenched alloy were also improved by the presence of β″ phase. Above 420°C, the effect of solid-solution hardening on the mechanical properties of the rolled alloys increased with increases in rolling temperature.

Keywords: aluminum alloys; heat treatment; rolling; mechanical properties; microstructure

1. Introduction

6XXX Al alloys are widely used as structural components in the automotive industry because of their good formability, corrosion resistance, weldability, and final mechanical properties [1–2].

Rolling is one of the most important plastic deformation techniques used to enhance the mechanical properties of Al alloys [3]. Several rolling processes have been investigated. For example, Panigrahi and Jayaganthan [4] rolled a 6063 Al alloy at cryogenic temperatures (cryorolling). Subsequently, they combined cryorolling and aging treatment to produce 6XXX Al alloys with ultra-high strength and ductility [5]. Kim *et al.* [6] produced a high-strength 6061 Al alloy using the differential speed rolling process. Furthermore, Rezaei *et al.* [7] fabricated a high-strength 6XXX Al alloy using a new method, called accumulative roll bonding (ARB) [8]. The tensile strength of the 6XXX Al alloys pro-

duced using these rolling techniques can be 2–3 times higher than the solution treatment state samples [4–7]. However, each method has its own limitations for commercial applications, such as the need for a cryogenic-temperature environment (in cryorolling), requirement for a special processing equipment (in differential speed rolling), and limited size (in ARB).

This study aimed to determine the effects of rolling temperature on the mechanical properties of 6XXX alloys using a normal symmetric rolling mill. Al–Mg–Si–Cu–Fe alloy was chosen as the starting material. The rolling temperature ranged from room temperature to solid-solution temperature of the 6XXX alloy.

2. Experimental

The raw material was a cast ingot of commercially available Al–Mg–Si–Cu–Fe alloy obtained from CITIC Dicastal Co., Ltd., Qinhuangdao, China. The chemical compo-

---

🙂 Springer

sition of the Al alloy was as follows: 1.03wt% Mg, 0.70wt% Si, 0.19wt% Cu, 0.18wt% Fe, 0.088wt% Cr, 0.062wt% Mn, 0.022wt% Ti, 0.02wt% Zn, 0.012wt% Ni, 0.022wt% Ga, and 0.01wt% V. The cast ingot was cut into 80 mm × 50 mm × 18 mm pieces. Prior to rolling, the plates were solid-solution treated at 560°C for 3 h and then cooled to room temperature following two different methods: rapid quenching to room temperature by immersing into water (water quenched, WQ) and slow cooling in a furnace (furnace cooled, FC). The WQ and FC alloy plates (each 50 mm wide) were rolled from 18 to 1 mm in eight passes (about 30% thickness reduction per pass and 94% thickness reduction in total). Between every rolling pass, the samples were reheated in a furnace at the prescribed rolling temperatures for 3 min. The rolling temperatures ranged from 20 to 560°C, the diameter of the rolling mill was 300 mm, and the rolling speed was 0.4 m/s. A schematic illustration of the production process is shown in Fig. 1.
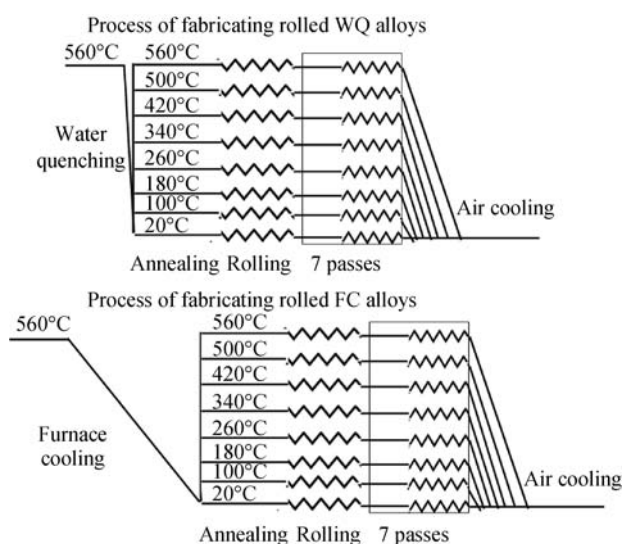

Fig. 1. Schematic illustration of the production process of rolled alloys.

The tensile-test samples were machined with the tensile axis parallel to the rolling direction. Tensile tests were performed at a strain rate of 4×10^{-4} s^{-1} using an Instron-5982-type test machine operated at a constant crosshead speed.

X-ray diffraction (XRD) analyses using Cu K$_\alpha$ radiation were performed to determine phases in the alloy. Light optical microscopy (OM) was used to observe the microstructures of the WQ and FC alloys. Metallographic samples were etched with 20vol% hydrofluoric acid, and the microstructures of the WQ, FC, and rolled alloys in the rolling direction–transverse direction (RD–TD) plane were observed by transmission electron microscopy (TEM). Samples were

prepared by mechanical grinding to a thickness of 0.15 mm, followed by thinning using a twinjet electropolishing unit in a solution of 10vol% acetic acid and 90vol% methanol at room temperature. Differential scanning calorimetry (DSC) was used to examine the transition temperature of the WQ alloy at a heating rate of 20°C/min. A sample weighing approximately 20 mg was placed in pans for DSC. After the tensile tests, fracture surfaces were observed by scanning electron microscopy (SEM) to determine the failure mode.

3. Results

3.1. Mechanical properties

The stress–strain curves of the WQ and FC alloys are shown in Fig. 2. The WQ alloy showed higher strength and elongation than the FC alloy. Fig. 3 shows the stress–strain curves of the rolled Al alloys deformed at different rolling temperatures, with a thickness reduction of 94%. Fig. 3(a) shows that the tensile strength of the 180°C rolling WQ alloy (513 MPa) was higher than that of any other rolled alloys and nearly twice as high as that of the solution treatment state samples.
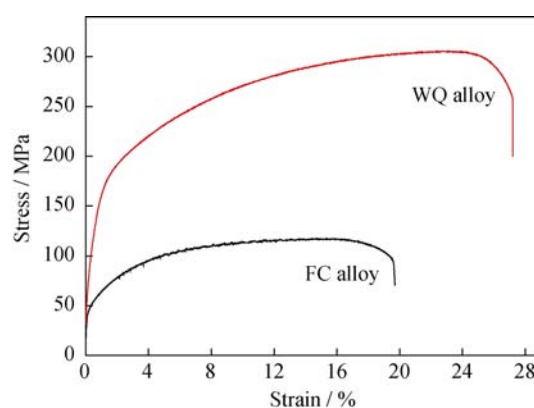

Fig. 2. Stress–strain curves of the WQ and FC alloys.

The stress–strain curve of the 180°C rolling WQ alloy shows a long extension of the work-hardening region. The maximum elongation of this sample reached 9.54%. By contrast, the 420°C rolling WQ alloy showed the lowest strength (195.71 MPa) and elongation (6.85%).

Slight differences were observed among the strengths of the 20°C, 180°C, and 560°C rolling FC alloys, as shown in Fig. 3(b). The lowest strength of the rolled FC alloys was observed at 420°C rolling temperature.

3.2. Structural evaluation

Fig. 4 shows the XRD patterns of the WQ, FC, and rolled alloys. Fig. 4(a) reveals that only an iron-rich (Al$_3$FeSi)

phase was formed in the WQ alloy. This iron-rich phase was observed in all rolled WQ alloys. However, Si and Mg_2Si peaks were observed in the 420°C rolling WQ alloy. When the rolling temperature reached 560°C, the Si phase was completely dissolved inside the Al matrix of the sample. However, the Mg_2Si phase could still be observed.

The FC samples showed the presence of Al–Cu, Al–Cu–Mg, and Al–Si–Mg–Fe compounds, and Mg_2Si in the Al–Mg–Si–Cu–Fe alloys, as shown in Fig. 4(b). Peak intensities of all the compounds weakened under the 94% rolling

reduction at room temperature. When the rolling temperature reached 560°C, only the Mg_2Si and Al–Si–Mg–Fe phases were observed in the alloys. OM micrographs of the WQ and FC alloys are shown in Fig. 5. Both alloys showed equiaxed grains, with their sizes varying from 70 to 120 μm.

Fig. 6 shows the TEM microstructures of the WQ and rolled WQ alloys. Numerous spherical-shaped phases, with sizes ranging from 100 to 200 nm, were found in the WQ alloy, as shown in Fig. 6(a). Energy dispersive spectroscopy (EDS) revealed that these phases were composed of Al, Si,
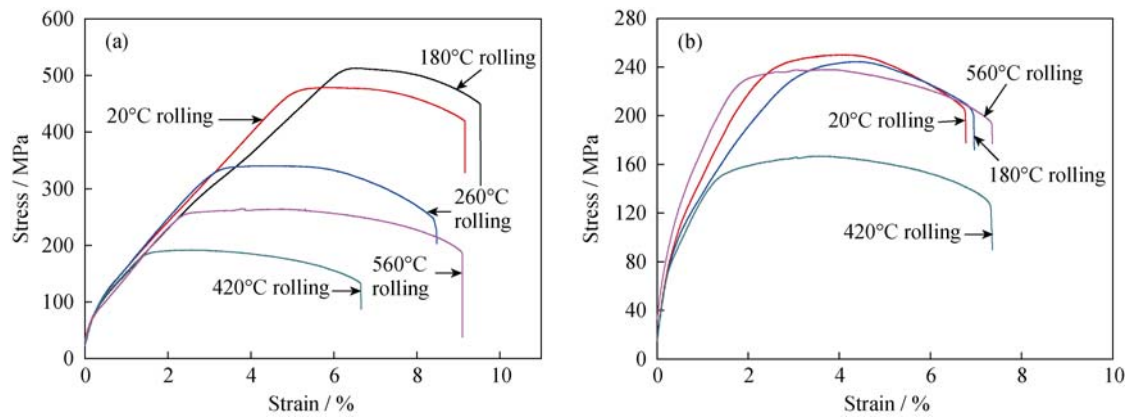

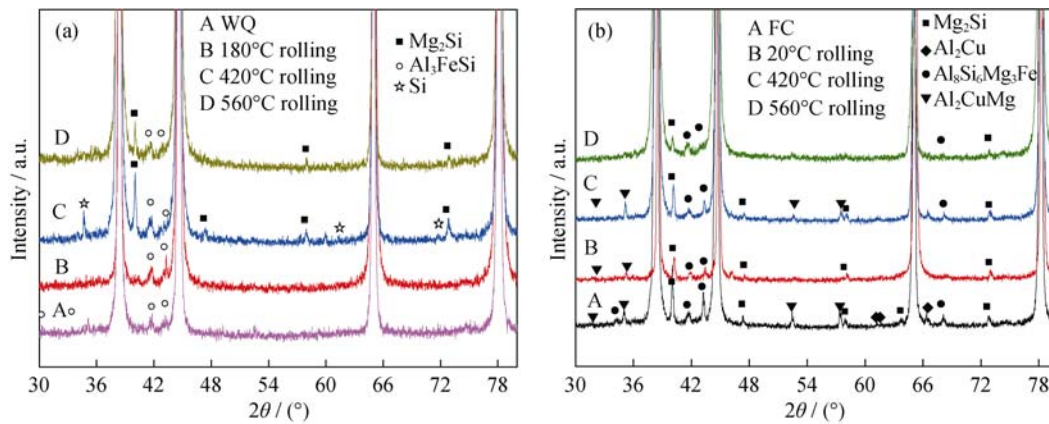**Fig. 3.   Stress–strain curves of the rolled WQ (a) and rolled FC (b) alloys.**

Fig. 4.   XRD patterns of the alloys: (a) WQ alloy and rolled WQ alloys; (b) FC alloy and rolled FC alloys.
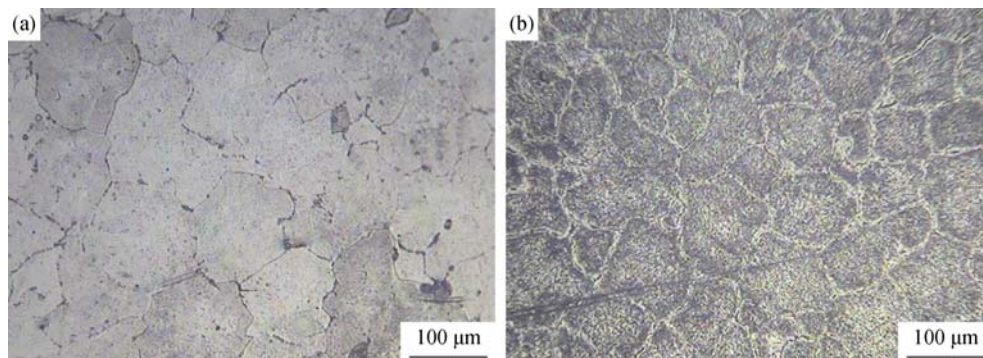

Fig. 5.   OM micrographs of the WQ alloy (a) and FC alloy (b) before rolling.
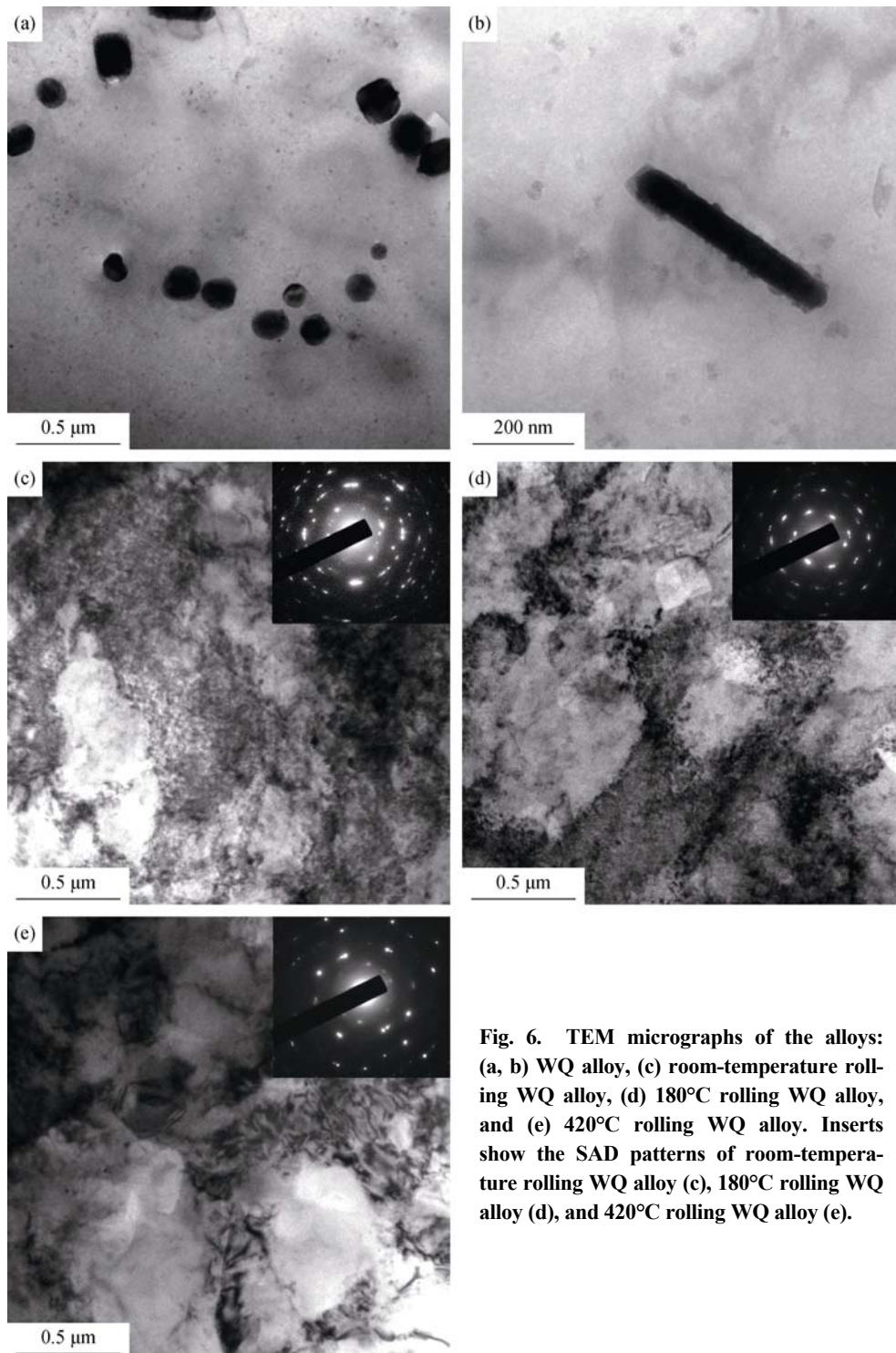
Fig. 6. TEM micrographs of the alloys: (a, b) WQ alloy, (c) room-temperature rolling WQ alloy, (d) 180°C rolling WQ alloy, and (e) 420°C rolling WQ alloy. Inserts show the SAD patterns of room-temperature rolling WQ alloy (c), 180°C rolling WQ alloy (d), and 420°C rolling WQ alloy (e).

and Fe. This finding corresponded to the iron-rich (Al_3FeSi) phase, which was also observed in the XRD patterns of the WQ alloys (Fig. 4(a)). Fig. 6(b) shows that the WQ alloy also contained rod-shaped phases consisting of Al, Si, Cu, and Fe, as detected by EDS. Figs. 6(c)–6(e) show the microstructural changes in the rolled WQ alloys at different rolling temperatures. Most grain boundaries of the room-temperature rolling (R-rolling) and 180°C rolling WQ alloys were not clear because of the presence of a large number of highly entangled dislocations. However, the corresponding selected area diffraction (SAD) patterns showed numerous small subgrains with high grain-boundary misorientation

angles in the two samples. As the rolling temperature was increased to 420°C, a reduction in the dislocation density and an increase in the cell boundaries were observed. A comparison of the SAD patterns between the 420°C rolling sample and low-temperature rolling alloys (Figs. 6(c) and 6(d)) indicated the development of a few small subgrains in the 420°C rolling alloys.

As can be seen from Fig. 7(a), a few spherical-shaped phases were observed in the FC alloys, but there were no rod-shaped phases. The spherical-shaped phase consisted of Al, Si, Fe, Mg, and Cu, as determined by EDS. Fig. 7(b) shows that the microstructure of the R-rolling FC alloy still contained a high density of dislocations and a large number of small subgrains.
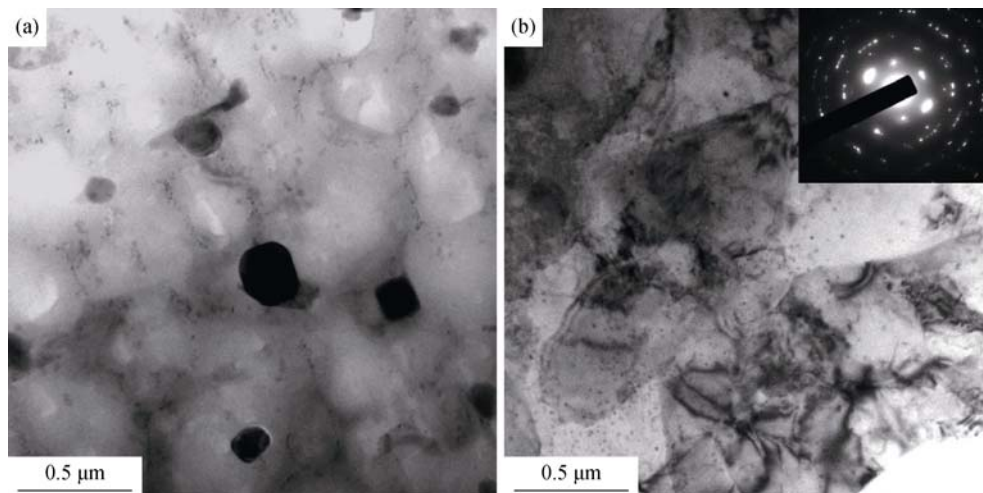

Fig. 7.   TEM micrographs of the FC alloy (a) and room-temperature rolling FC alloy (b). Insert in (b) shows the SAD pattern of room-temperature rolling FC alloy.

4. Discussion

4.1. Strengthening mechanism

Fig. 8 demonstrates the variations in the tensile strength of the WQ, FC, and rolled alloys. Compared with the tensile strength of fully annealed pure Al (80 MPa [9]), the WQ and FC alloys were clearly stronger. The solid-solution-treated commercial Al–Mg–Si–Cu–Fe alloys were processed by water quenching and furnace cooling; both the WQ and the FC alloys showed nearly similar grain sizes (Fig. 5) and nearly no dislocation (Figs. 6(a) and 7(a)). The presence of some iron-rich particles, with sizes ranging from 100 to 200 nm, was observed in both alloys because of the poor solubility of Fe in Al. Thus, the main strengthening mechanism of the FC alloy was particle reinforcement by the iron-rich phase. For the WQ alloy, the effect of solid-solution strengthening was much more important than that of particle reinforcement. Thus, the main strengthening mechanism of the WQ alloy was solid-solution strengthening.

The R-rolling WQ alloy showed higher tensile strength than the WQ alloy. Fig. 6(c) shows numerous small subgrains and dislocations in the R-rolling WQ alloy. The main strengthening mechanisms of the R-rolling WQ alloy were solid-solution strengthening, grain boundary hardening, and strain hardening by the dislocations.

Fig. 8 shows that the peak tensile strength of the rolled WQ alloys occurred at 180°C rolling temperature. The fabrication procedure of this sample included the following steps: aging at 180°C for 3 min + (rolling at 180°C + aging at 180°C for 3 min) × 7 + rolling at 180°C. Thus, in addition to the strain imposed on the rolling process, the short aging period at 180°C may also play a role in the evolution of the mechanical properties.
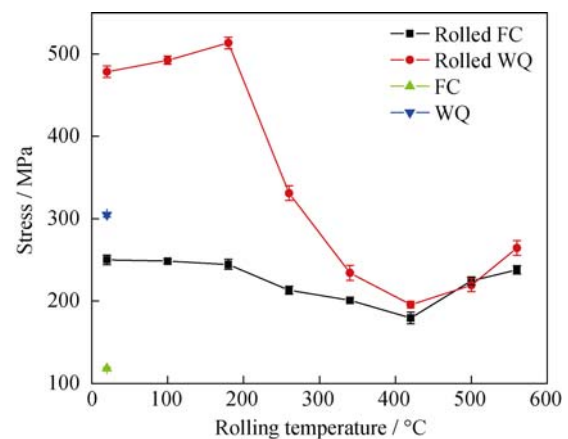

Fig. 8.   Tensile strength of the WQ, FC, rolled WQ, and rolled FC alloys at various rolling temperatures.

Edwards *et al.* [10] found that the precipitation sequence of the solid-solution-treated 6XXX Al alloy was as follows:

clusters of Si Atoms (SSSS) → Guinier–Preston (GP) zones → β″ → β′ → β (Mg_2Si). As demonstrated by Buha *et al.* [11], the GP zones essentially represent disordered solute atom aggregates that are fully coherent with the matrix. The presence of the semicoherent β″ precipitates, which evolved from the GP zones, was associated with the optimal mechanical properties of Al–Mg–Si alloys. When the β′ and β equilibrium phases were formed, the alloys exhibited reduced mechanical properties.

Fig. 9 shows the DSC curves for the R-rolling WQ and 180°C rolling WQ alloys. The R-rolling WQ alloy had three exothermic peaks: peak 1 at ~160°C, peak 2 at ~235°C, and peak 3 at ~380°C. These peaks were associated with the formation of GP zones, β″ precipitates, and Mg_2Si precipitates, respectively, as reported by Panigrahi and Jayaganthan [12]. The 180°C rolling WQ alloy showed peaks at lower temperatures than the R-rolling WQ alloy. This phenomenon indicated the precipitation of the GP zones and β″ phase during the rolling and short-time aging at 180°C. When the WQ alloy was rolled at room temperature, the sample did not receive sufficient thermal energy to precipitate the solutes from the solid solution. However, nanoscale particles precipitated readily and were distributed within the grains following a severe deformation caused by the presence of numerous dislocations, which served as preferential sites for precipitation. During the short aging time at 180°C, β″ phase was formed. Furthermore, according to Nageswara and Jayaganthan [13] and Kang *et al.* [14], dynamic precipitation during the warm deformation process also led to the precipitation of β″ phase. Fig. 6(d) shows the high density of dislocations and small subgrains remaining in the sample. Thus, the significant enhancement in the strength of the 180°C rolling WQ alloy can be attributed to the cumulative effect of precipitation hardening, boundary hardening, and strain hardening by the dislocations.
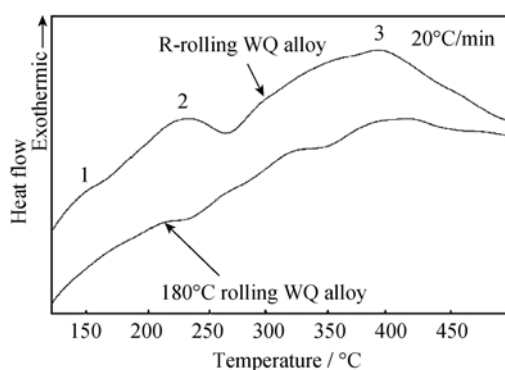

Fig. 9. DSC plots for the heat flow of precipitation reactions in the room temperature rolling WQ alloy and 180°C rolling WQ alloy.

The tensile strength of the rolled WQ alloy decreased with an increase in the rolling temperature from 180°C to 420°C, as shown in Fig. 8. Strength of the rolled WQ alloys was lower than that of the WQ alloy when the rolling temperature was >340°C. Fig. 4(a) shows the equilibrium of the Si and Mg_2Si phases observed in the 420°C rolling WQ alloy. No β″ phase and solid-solution strengthening were observed in the sample. The effect of grain boundary strengthening and dislocations decreased with increasing rolling temperature (Fig. 6), which resulted in the low strength of the 420°C rolling WQ alloy.

The tensile strength of the rolled WQ alloy increased with increasing rolling temperature above 420°C, which can be attributed to solid-solution strengthening at high temperatures. Fig. 4(a) shows the XRD peaks of Mg_2Si for the 560°C rolling WQ alloy, which can be attributed to the air cooling of the sample after the last rolling pass. However, the intensity of these Mg_2Si peaks was much lower than those of the 420°C rolling WQ alloy.

The effects of rolling temperature on the tensile strength of the rolled FC alloy differed from those of the rolled WQ alloy. The tensile strength of the rolled FC alloy decreased with increasing rolling temperature up to 420°C. The main strengthening mechanisms underlying the low-rolling-temperature FC alloys were boundary hardening and strain hardening by the dislocations. The subgrain size and dislocation density decreased with increasing rolling temperature. Above 420°C, the tensile strength of the rolled FC alloy increased with increasing rolling temperature. Fig. 4(b) shows that some equilibrium phases disappeared in the 560°C rolling FC alloy. Thus, the effect of solid-solution strengthening on the strength of the rolled FC alloy increased with increasing temperature above 420°C.

4.2. Ductility of alloys

Fig. 10 shows that the tensile elongation of the WQ alloy was higher than that of the FC alloy. Figs. 11(a) and 11(b) show the fracture surfaces of the WQ and FC alloys. Compared with the fracture surface of the WQ alloy, the fracture surface of the FC alloy contained micrometer-sized particles, which were considered as the equilibrium phases that formed during the annealing process. These equilibrium phases caused a premature failure in the FC alloy during the tensile process.

In the present study, all rolled alloys showed a higher tensile elongation than the cryorolled 6XXX Al alloys [13−14]. According to Zhu and Liao [15] and Kim and Yoo [16], ductility was controlled by two material parameters: work hardening and strain-rate sensitivity. High values of these parameters helped delay the onset of the localized de-

formation ("necking") under tensile stress, thereby improving ductility. The R-rolling and warm rolling alloys showed a high tensile elongation caused by high work hardening, as shown in Fig. 3. Compared with the cryorolled alloys, the warm rolling alloys showed a lower dislocation density, which can be attributed to dynamic recovery and/or recrystallization. For the studied alloys, during tensile testing, new dislocations were formed; these interacted with the pre-existing dislocations to form tangles that increased the dislocation density and work-hardening capacity. By contrast, the cryorolled samples already had a considerable amount of pre-existing dislocations. During tensile testing, destruction and rearrangement of pre-existing dislocations decreased the dislocation density and work-hardening capacity, thereby reducing elongation.
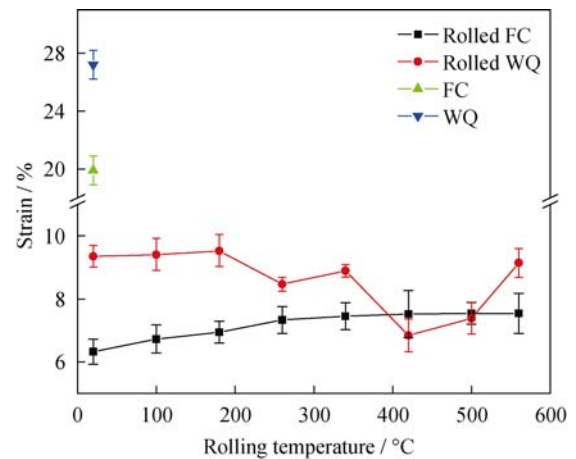

Fig. 10.   Tensile elongation of the WQ, FC, rolled WQ, and rolled FC alloys at various rolling temperatures.
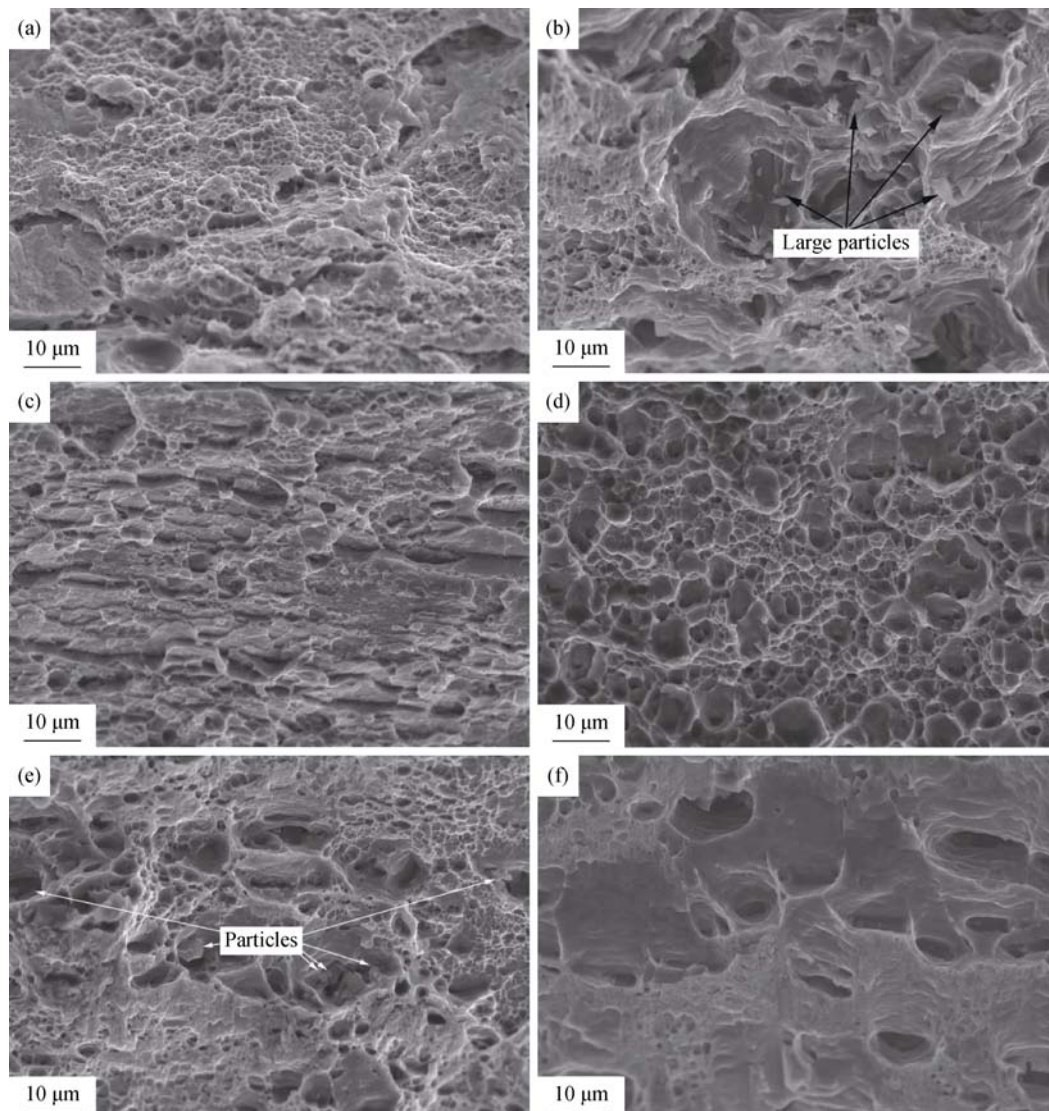

Fig. 11.   Fracture surfaces after tensile test: (a) WQ, (b) FC, (c) 180°C rolling WQ, (d) 560°C rolling WQ, (e) R-rolling FC, and (f) 560°C rolling FC alloys.

Nanoscale β″ phase was introduced into the Al matrix of the 180°C rolling WQ alloy. Zhao *et al.* [17] found that the precipitate phases in Al alloys help in the accumulation of dislocations during the deformation and then enhance the work-hardening capacity and elongation of alloys. Thus, the high elongation of the 180°C rolling WQ alloy can also be attributed to the presence of β″ phase.

The fracture surface of the 180°C rolling WQ alloy showed elongated dimples (Fig. 11(c)), whereas that of the 560°C rolling WQ alloy showed equiaxed dimples (Fig. 11(d)). Both the microstructures of the fracture surfaces corresponded to the high tensile elongation. The low elongation of the 420°C rolling WQ alloy can be attributed to the emergence of Si and Mg_2Si equilibrium phases.

Fig. 10 shows that the tensile elongation of the rolled FC alloys increased with increasing rolling temperature. The increase in tensile elongation below 420°C can be attributed to the softening effect caused by high deformation temperatures and that above 420°C to the softening effect and the solid solution of the impurity phase at high temperatures. Similar to the fracture surface of the FC alloy, micrometer-sized particles appeared in the dimples of the R-rolling FC alloy, as shown in Fig. 11(e). On the other hand, large particles were not formed on the fracture surface of the 560°C rolling FC alloy, as shown in Fig. 11(f).

5. Conclusions

The effect of rolling temperature on the mechanical properties of Al–Mg–Si–Cu–Fe alloys was studied in detail. The following conclusions were made:

(1) Peak values corresponding to the tensile elongation and strength of the rolled WQ alloys were obtained at 180°C rolling temperature. The strengthening mechanism of the 180°C rolling WQ alloy involved the cumulative effect of precipitation hardening, boundary hardening, and strain hardening by dislocations. The high tensile elongation can be attributed to the high work-hardening capability of the 180°C rolling WQ alloy.

(2) Two peaks corresponding to the strength of the rolled FC alloy were observed at 20°C and 560°C rolling temperatures. Boundary hardening and strain hardening induced by dislocations were the strengthening mechanisms of the FC alloy rolled at room temperature. On the other hand, the main strengthening mechanism of the 560°C rolling FC alloy was solid-solution strengthening.

(3) The poorest mechanical properties of the rolled WQ

and FC alloys were obtained at 420°C rolling temperature, which should thus be avoided in commercial production.

Acknowledgements

References

[1]   N. Geoffroy, E. Vittecoq, A. Birr, F. de Mestral, and J.M. Martin, Fatigue behaviour of an arc welded Al–Si–Mg alloy, *Scripta Mater.*, 57(2007), No. 4, p. 349.

[2]   Y.L. Ji, H. Zhong, P. Hu, and F. Guo, Use of thermodynamic calculation to predict the effect of Si on the ageing behavior of Al–Mg–Si–Cu alloys, *Mater. Des.*, 32(2011), No. 5, p. 2974.

[3]   D. Singh, P.N. Rao, and R. Jayaganthan, Microstructures and impact toughness behavior of Al 5083 alloy processed by cryorolling and afterwards annealing, *Int. J. Miner. Metall. Mater.*, 20(2013), No. 8, p. 759.

[4]   S.K. Panigrahi and R. Jayaganthan, Effect of rolling temperature on microstructure and mechanical properties of 6063 Al alloy, *Mater. Sci. Eng. A*, 492(2008), No. 1-2, p. 300.

[5]   S.K. Panigrahi and R. Jayaganthan, A study on the combined treatment of cryorolling, short-annealing, and aging for the development of ultrafine-grained Al 6063 alloy with enhanced strength and ductility, *Metall. Mater. Trans. A*, 41(2010), No. 10, p. 2675.

[6]   W.J. Kim, J.Y. Wang, S.O. Choi, H.J. Choi, and H.T. Sohn, Synthesis of ultra high strength Al–Mg–Si alloy sheets by differential speed rolling, *Mater. Sci. Eng. A*, 520(2009), No. 1-2, p. 23.

[7]   M.R. Rezaei, M.R. Toroghinejad, and F. Ashrafizadeh, Effects of ARB and ageing processes on mechanical properties and microstructure of 6061 aluminum alloy, *J. Mater. Process. Technol.*, 211(2011), No. 6, p. 1184.

[8]   Y. Saito, N. Tsuji, H. Utsunomiya, T. Sakai, and R.G. Hong, Ultra-fine grained bulk aluminum produced by accumulative roll-bonding (ARB) process, *Scripta Mater.*, 39(1998), p. 1221.

[9]   C.Y. Liu, Q. Wang, Y.Z. Jia, B. Zhang, R. Jing, M.Z. Ma, Q. Jing, and R.P. Liu, Evaluation of mechanical properties of 1060-Al reinforced with WC particles via warm accumulative roll bonding process, *Mater. Des.*, 43(2013), p. 367.

[10] G.A. Edwards, K. Stiller, G.L. Dunlop, and M.J. Couper, The precipitation sequence in Al–Mg–Si alloys, *Acta Mater.*, 46(1998), No. 11, p. 3898.

[11] J. Buha, R.N. Lumley, A.G. Crosky, and K. Hono, Secondary precipitation in an Al–Mg–Si–Cu alloy, *Acta Mater.*, 55(2007), No. 9, p. 3015.

[12] S.K. Panigrahi and R. Jayaganthan, Influence of solutes and second phase particles on work hardening behavior of Al 6063 alloy processed by cryorolling, *Mater. Sci. Eng. A*, 528(2011), No. 7-8, p. 3147.

[13] P. Nageswara and R. Jayaganthan, Effects of warm rolling and ageing after cryogenic rolling on mechanical properties and microstructure of Al 6061 alloy, *Mater. Des.,* 39(2012), p. 226.

[14] U.G. Kang, H.J. Lee, and W.J. Nam, The achievement of high strength in an Al 6061 alloy by the application of cryo-genic and warm rolling, *J. Mater. Sci.*, 47(2012), p. 7883.

[15] Y.T. Zhu and X.Z. Liao, Nanostructured metals: retaining ductility, *Nat. Mater.*, 3(2004), p. 351.

[16] W.J. Kim and S.J. Yoo, Enhanced ductility and deformation mechanisms of ultrafine-grained Al–Mg–Si alloy in sheet form at warm temperatures, *Scripta Mater.*, 61(2009), No. 2, p. 125.

[17] Y.H. Zhao, X.Z. Liao, S. Cheng, E. Ma, and Y.T. Zhu, Si-multaneously increasing the ductility and strength of nanos-tructured alloys, *Adv. Mater.*, 18(2006), No. 17, p. 2280.